Research Article

Microstrip Reflectarray Design for 26 GHz

Israa sh. Aqrab[1*], Hülya Gökalp Clarke[2*], Mohammed Alhennawi[3*]

[1] Ondokuz Mayıs University, Faculty of Engineering, Departmant of Electric and Electronic, Samsun, Turkey, (ORCID: 0000-0002-7523-6347), israashihab83@gmail.com
[2] Ondokuz Mayıs University, Faculty of Engineering, Departmant of Electric and Electronic, Samsun, Turkey, (ORCID: 0000-0002-3102-2136), hulya.gokalp@omu.edu.tr
[3] Ondokuz Mayıs University, Faculty of Engineering, Departmant of Electric and Electronic, Samsun, Turkey, (ORCID: 0000-0002-5398-1741), mohammed.hennawi@gmail.com

(First received September 05, 2022 and in final form December 16, 2022)

Reference: Aqrab I., Clarke H. G., Alhennawi M. Microstrip Reflectarray Design for 26 GHz. The European Journal of Research and Development,2(4), 169-177.

Abstract

This paper presents microstrip reflectarray design using variable size unit cell approach for 26 GHz, and investigates the effect of feed antenna distance to the surface. The unit cell structure is made up of a 1.5 mm foam layer (εr=1.37) and a 0.787 mm substrate layer (εr=2.2) between the ground and reflective layers. Two arrays of 14λx14λ in size were designed to reflect the incoming wave in the θ=25º direction; the distance to the feed was 160 mm in one design and 320 mm in the other design. Simulation results show gain of 30.2 dBi for the former and 29.8 dBi for the latter. 3-dB gain bandwidths were 11 % and 14 %, respectively.

Keywords: *Microstrip reflect array, Unit cell, Gain, Bandwidth*

1. Introduction

Direct line of site (LOS) for long range microwave communications is often not feasible because a number of obstacles may block the LOS path and degrade the quality of the communication, limiting the coverage [1]. Reflectarray Surfaces (RS) that have LOS links to both transmitters and receivers can overcome these challenges by reflecting incoming signals with a high gain beam and focusing the energy in a specific direction, allowing the signal to reach its destination by an alternative path [2].

The feed antenna is usually horn-shaped. Behind the unit cells there is usually a ground plane; the incoming wave is reflected in the direction of the receiver. An appropriate reflection phase distribution across the surface aperture can be used to compensate difference in phase delays due to different path lengths from the feed antenna to each unit cell, and to focus the incoming wave from the feed antenna into a

highly directive beam)[3-4]. For this, the phase distribution on the reflector aperture must be varied. In [5], passive reflectors and an active repeater were used to improve coverage at 28 GHz, hence enhancing the strength of the received signal and extending the range of mmWave signals.

Reflection coefficient and penetration loss for common building materials at 28 GHz are presented in [6]. Measurements in and around buildings show that outdoor building materials are excellent reflectors, with the largest measured reflection coefficient of 0.896 for tinted glass. Indoor building materials, were found to be less reflective. High reflectivity of the materials at 28 GHz means high penetration loss. Therefore, if no measures taken, signals originating from outdoors cannot directly be used indoors. In [7], far-field path loss was derived by using physical-optical techniques and the reason why the surface consists of many elements that individually act as diffuse scatterers but can coherently radiate the signal in the desired direction with a given beam width is explained. In [8], a RIS proof-of-concept prototype was developed, and its potential benefits in practice under realistic wireless communication conditions were extensively evaluated. Specifically, a 160-element RIS operating at 5.8 GHz bandwidth was designed, fabricated, and accurately measured in the anechoic chamber. The results show that the developed RIS system can achieve an SNR gain of about 20 dB when both the transmitter and receiver use directional antennas located at a distance of 5-10 m from the RIS

Two microstrip reflectarray designs based on variable size unit cells for 10 GHz was presented in [9]. One design uses a 3-layer unit cell with a polygonal patch and the other design uses a unit cell with a single-layer square loop patch. The advantage of the multilayer structure is a wider gain bandwidth. The simulation results show that the 3-dB bandwidth gain fraction for the 3-layer reflective array structure is about 22%, compared with a bandwidth fraction of 12% for the single-layer structure.

The objective of this work is to design reflectarray surfaces for 26 GHz that is capable of reflecting incident waves with high gain in a specific direction. Two reflectarray surfaces were designed to reflect the incoming waves in the $\theta = 25°$ direction. The distance to the feed antenna was 160 mm for one surface and 320 mm for the other surface. We investigated the effect of the distance to the source antenna on the peak gain of the reflected beam and 3-dB gain bandwidth.

2. Materials and Methods

The overall design of the reflector surface is based on the design of a unit cell that allows an acceptable range of phase shifts. The unit cells on the aperture should have a progressive phase distribution that compensates for the difference in phase shifts arising from different spatial delays from phase center to the n^{th} element. Required phases on the reflector aperture can be calculated as follows.

$$\emptyset(x_n, y_n) = k_0(r_{k,n} - \sin\theta_0\,(x_n \cos\varphi_0 + y_n \sin\varphi_0)) \quad (1)$$

Where, (x_n,y_n) is the position of n^{th} element on the reflectarray surface, (θ^0,φ^0) represents the direction of the reflected beam where θ and φ are elevation and azimuth angles, respectively, and k_0 is the wavenumber at the center frequency, and $r_{k,n}$ is the distance from the feed center to n^{th} element position on the reflectarray surface.

2.1. Unitcell Design

In the current work, a variable element size approach was used to control the reflection phase of the unit cells. Computer Simulation Technology (CST) (Microwave Studio Suite) was used to design and simulate the unit cells and arrays. MATLAB was used to calculate appropriate reflection phases (i.e., element sizes) for each element on the array aperture and to transfer the reflection phase results as a function of element position to CST to enable automated building of the reflectarray in CST. The Antenna Magus program was used to design a source antenna to illuminate the array in CST simulations.

The unit cell design is the first step in the design. Once the unit cell structure is formed, simulations are carried out to obtain reflection characteristics of the cell versus element size. The unit cell design that gave a reflection phase range of more than 280º were used in the array designs. A wide range of reflection phases is necessary to reflect the incoming wave as a highly directive beam in a specified direction. Figure 1 shows the structure of the unit cell designed. The top layer of the unit cell consists of a metallic square loop of inner length L1= 5mm and outer length L=6mm printed on a Roger RT 5880 substrate (with a thickness of 0.787 mm, εr = 2.2, and tanδ = 0.0009) and separated from the ground plane by a 1.5 mm thick foam layer (εr = 1.37). Table 1 lists the dimensions of the unit cell.

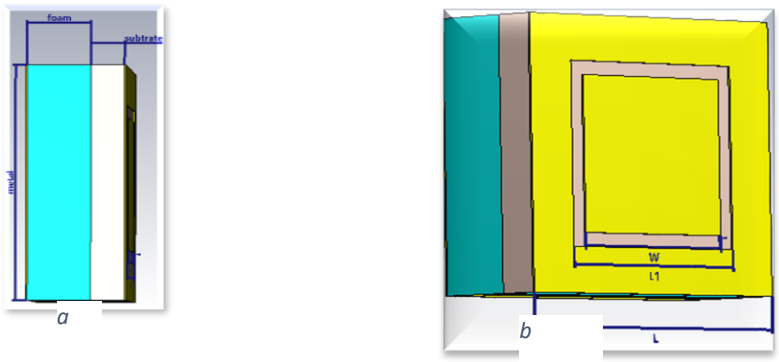

Figure 1: Unitcell design: (a) side view; (b)top view

Table 1:Unitcell Parameters(mm)

L	L1	Foam	Subtrate
6	5	1.5	0.787

Size of the square patch on the top layer was varied to change the reflection phase. A Floquet port was used to excite and determine the reflection properties (magnitude and phase values) of the unit cells for different patch sizes. The Floquet port was placed at an exact distance of half a wavelength at 26 GHz from the top of the unit cells. The edge length w of the square patch was varied from 0.2 mm to 3.4 mm. Fig (2) illustrates reflection characteristics of the unit cell versus patch size. The magnitude of the reflection coefficient was greater than 0.955 for all the patch sizes. The range of reflection phase variation is about 282º. This reflection phase range was thought to be wide enough to achieve the required reflection phase at each individual element on the aperture and to compensate for the phase differences caused by the distances between the source and the array elements on the reflector surface

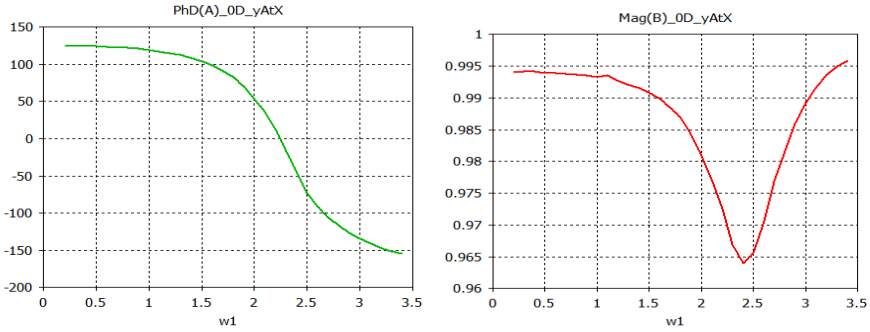

(a) (b)

Figure 2: *Reflection phase versus unit element size: (a)length vs reflected phase; (b) leght vs magnitude*

2.2. Reflectarray Design

For the current work, the aim was to design two arrays of 14λx14λ in size and that reflect the incoming wave in the θ=25º direction. In order to reflect incoming wave as a highly directive beam in a specific direction, it is necessary that each unit cell in the aperture compensates for the differences in spatial phase delay from source to the array surface. This is achieved by reflecting the incoming wave with an appropriate reflection phase at each unit cell.

The required phase distribution, i.e., element size, on the array aperture is calculated in MATLAB. The phase shift versus cell size data table was obtained from the unit cell design phase in CST, and was used to determine the appropriate cell dimensions

for each element position on the array aperture. Figure 3 shows the mask plots for the reflectarrays for the reflection direction of θ=25º for 160 mm and 320 mm feed antenna spacing.

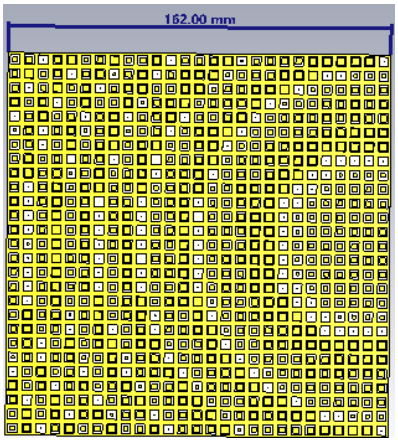

Figure 3: Mask of the array for reflection in the direction of ϑ =25° at antenna distance 160 mm

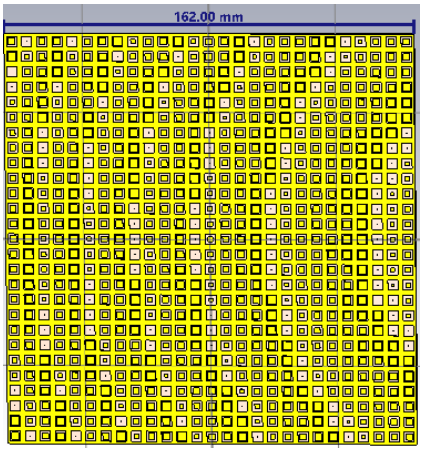

Figure 4: Figure 3 Mask of the array for reflection in the direction of ϑ =25° at antenna distance 320 mm

2.3. Far-field Radiation Analysis of the Arrays

A horn antenna was designed by using the Antenna Magus program, and it was used for illuminating the reflectarray in the CST simulations. The geometry of the horn antenna is shown in Fig. 5, and the dimensions are given in the caption. The horn antenna was analyzed in CST, giving s11 below -18 dB from 22 GHz to 30 GHz, a gain of 18 dBi at 26 GHz, and half power beam width of about 16°

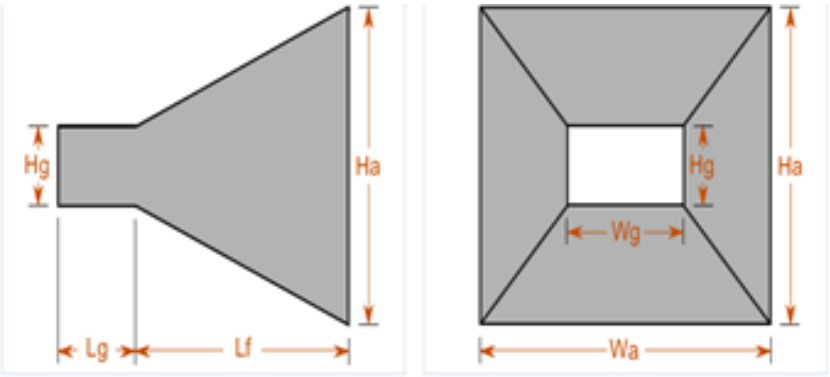

Figure 5: Dimensions of the horn antenna (in mm): Hg=4.526; Wg=9.051; Lg=11.53; Lf=34.73; Ha=31.67; Wa=41.20

3. Results

The two-dimensional radiation patterns on the E-plane for 26 GHz are shown in Fig. 6 and 7. It can be seen that both arrays can reflect the incident wave as a pencil beam with high gain in the desired direction of 25° (θ = 25°). The array with feed antenna spacing of 160 mm has a gain of 30.4 dBi at θ = 25° (Fig. 6a), and a sidelobe level of -16.9 dB. The corresponding values for the 320 mm antenna spacing are 29.8 dBi and -20 dB , respectively (Fig.7a) .

The simulations were performed at different frequencies to determine the gain bandwidth of the proposed arrays. According to the plots of gain versus frequency, the peak gain is 30.3 dBi at 26.3 GHz and 3-dB gain bandwidth is about 10.5 % for the antenna spacing of 160 mm (Fig.6.b). Peak gain of 29.8 dBi is obtained at 25.3 GHz for the antenna spacing of 320 mm (Fig. 7b), and 3-dB gain bandwidth is about 14%.

The spatial power density incident on the n^{th} element is:

$$s_n^k = P_T G_T(\hat{r}_n^k)/4\pi r_{k,n}^2 \quad (2)$$

where P_T is the total power applied by the transmitter to the transmit antenna, $G_T(\hat{r}_n^k)$ is the transmit antenna gain in the defined direction $\hat{r}_n^k$, and $r_{k,n}$ refers to the distance from the transmitter to the n^{th} element. The power captured by the n^{th} element can be found by multiplying the element's effective aperture and the power density incident on the element and

$$P_k = S_n^k A_e(-\hat{r}_n^k) \quad (3)$$

Where A_e(-^$r_{k,n}$) is the element's effective aperture in the transmitter's direction. With distance to the feed antenna, $G_T(\hat{r}_n^k)$ and $A_e(-\hat{r}_n^k)$ over the surface aperture will change. The footprint of the half-power-beam-width of the feed antenna on the reflect array surface will be roughly 45mm x 45 mm for the surface with 160 mm distance to the feed antenna and 90 mm x 90 mm for the other surface. Although areas of both footprints are smaller than the reflectarray aperture, the power density of the incoming wave on the

surface will be more concentrated for the shorter antenna spacing, and therefore the amount of power flux intercepted and reflected by the reflectarray will be greater. This can explain the difference of 0.4 dB between the peak gains of the reflectarrays. The gain of the receive antenna in the far field can be assumed to be constant over the reflectarray. Assuming that the same fraction (q, q<1) of the power incident on the surface aperture is reflected towards the receiver, the received power can be expressed as:

$$P_R = P_T\, G_T(\hat{r}_n^k) G_R A_e(-\hat{r}_n^k) \mathrm{q} / \left(4\pi r_{k,n} r_{a,n}\right)^2 \qquad (4)$$

Where $r_{a,n}$ is the distance of n^{th} element to the receiver

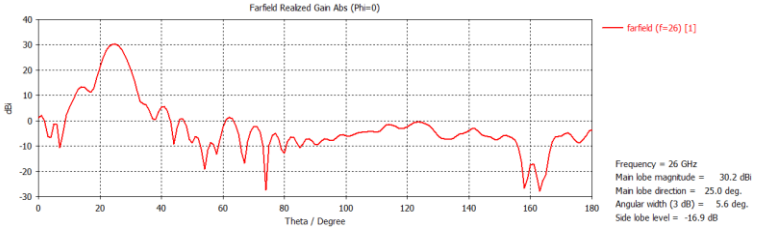

Figure 6(a): Radiation patterns for the source distance of 160 mm

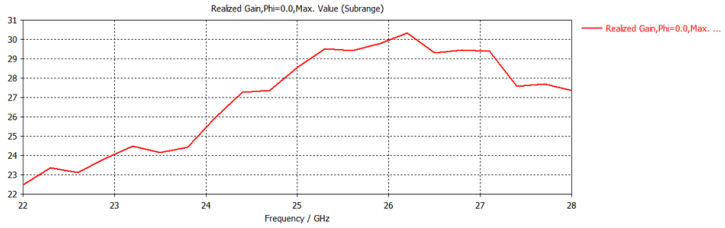

Figure 6(b): Gain versus frequency for source distance of 160 mm

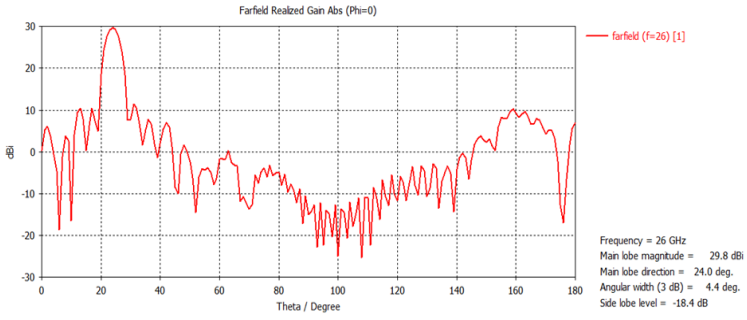

Figure 7(a): Radiation pattern for the source distance of 320 mm

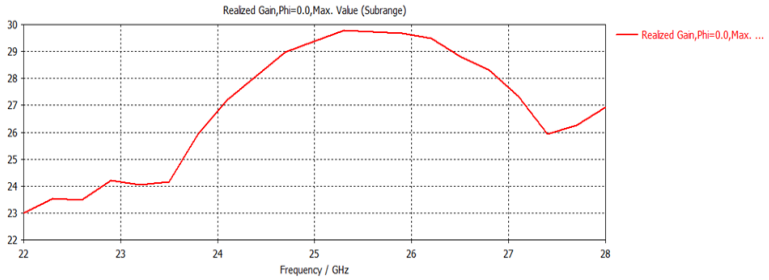

Figure 7(b): Gain versus frequency for source distance of 320 mm

4. Discussion and Conclusion

Two reflector arrays were designed to reflect the incoming waves in the θ = 25° direction; one with 160 mm distance to the feed antenna and the other with 320 mm distance to the feed. Both arrays are capable of reflecting the incoming wave as a pencil beam with high gain in the direction of θ = 25°. The first surface gave 30.3 dB peak gain at 25.5 GHz and about 10% 3-dB gain bandwidth. The peak gain of about 29.8 dBi at 26.3 GHz and a bandwidth of 14% were obtained f or the other surface with 320 mm distance to the source.

References

[1] D. Gunduz, D. B. Kurka, M. Jankowski, M. M. Amiri, E. Ozfatura, and S. Sreekumar, "Communicate to Learn at the Edge," *IEEE Communications Magazine*, vol. 58, no. 12, pp. 14–19, Dec. 2020, doi: 10.1109/MCOM.001.2000394.

[2] J. Zhao, "A Survey of Intelligent Reflecting Surfaces (IRSs): Towards 6G Wireless Communication Networks," Jul. 2019, [Online]. Available: http://arxiv.org/abs/1907.04789

[3] M. Chen, Z. Yang, W. Saad, C. Yin, H. V. Poor, and S. Cui, "A Joint Learning and Communications Framework for Federated Learning over Wireless Networks," *IEEE Trans Wirel Commun*, vol. 20, no. 1, pp. 269–283, Jan. 2021, doi: 10.1109/TWC.2020.3024629.

[4] S. Gong *et al.*, "Toward Smart Wireless Communications via Intelligent Reflecting Surfaces: A Contemporary Survey," *IEEE Communications Surveys and Tutorials*, vol. 22, no. 4, pp. 2283–2314, Oct. 2020, doi: 10.1109/COMST.2020.3004197.

[5] O. Ozdemir, F. Erden, I. Guvenc, T. Yekan, and T. Zarian, "28 GHz mmWave Channel Measurements: A Comparison of Horn and Phased Array Antennas and Coverage Enhancement Using Passive and Active Repeaters," Jan. 2020, [Online]. Available: http://arxiv.org/abs/2002.00121

[6] H. Zhao *et al.*, "28 GHz Millimeter Wave Cellular Communication Measurements for Reflection and Penetration Loss in and around Buildings," 2013.

[7] O. Ozdogan, E. Bjornson, and E. G. Larsson, "Intelligent Reflecting Surfaces: Physics, Propagation, and Pathloss Modeling," *IEEE Wireless Communications Letters*, vol. 9, no. 5, pp. 581–585, May 2020, doi: 10.1109/LWC.2019.2960779.

[8] G. C. Trichopoulos *et al.*, "Design and Evaluation of Reconfigurable Intelligent Surfaces in Real-World Environment," *IEEE Open Journal of the Communications Society*, vol. 3, pp. 462–474, 2022, doi: 10.1109/OJCOMS.2022.3158310.

[9] M. ALHENNAWİ and H. G. CLARKE, "Designing Wideband Microstrip Reflectarrays for 10 GHz," *European Journal of Science and Technology*, Jan. 2022, doi: 10.31590/ejosat.1040838.

[10] "Cst Studio Suite. Electromagnetic Field Simulation Software Electromagnetic Field Simulation Software, 2021."